Pure Appl. Chem., Vol. 84, No. 4, pp. 1005–1025, 2012.
http://dx.doi.org/10.1351/PAC-CON-11-09-22

Tetrathiafulvalene vinylogues as versatile building blocks for new organic materials*

Yuming Zhao‡, Guang Chen, Karimulla Mulla, Ilias Mahmud, Shuai Liang, Prateek Dongare, David W. Thompson, Louise N. Dawe, and Stephen Bouzan

Department of Chemistry, Memorial University of Newfoundland, St. John's, Newfoundland A1B 3X7, Canada

Abstract: Although tetrathiafulvalene (TTF) and its derivatives have been extensively studied as important organic electronic materials over the past half century, tetrathiafulvalene vinylogues (TTFVs) still remain a relatively underdeveloped branch in the family of TTF derivatives. Our recent work has investigated the synthesis and characterization of a class of diphenyl-substituted TTFVs carrying alkynyl functionality. The unique conformational and redox properties of such TTFV derivatives along with the versatile chemistry enabled by acetylenic groups (e.g., metal-catalyzed coupling and click reactions) have led us to a variety of functional molecular architectures ranging from oligoynes, polymers, and molecular tweezers, to macrocycles. Property studies of these new TTFV-based molecular materials point to appealing applications in molecular electronics and optoelectronics.

Keywords: chemosensors; click reaction; π-conjugation; cross-coupling; cycloaddition; electrochromism; polymers; redox; tetrathiafulvalene.

INTRODUCTION

Despite its relatively simple molecular structure, tetrathiafulvalene (TTF) has attracted enormous attention since shortly after its first synthesis in the early 1970s by Wudl and co-workers [1]. As a non-aromatic sulfur-containing heterocyclic compound, TTF presents an excellent organic π-electron donor that readily releases two electrons upon oxidation to yield stable radical cation ($TTF^{+\bullet}$) and dication (TTF^{2+}) species as a result of the gaining of aromaticity on the dithiolium ring (Fig. 1) [2].

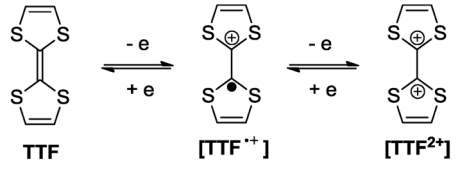

Fig. 1 Reversible electron-transfer reactions of TTF.

Pure Appl. Chem.* **84, 861–1112 (2012). A collection of invited papers based on presentations at the 14th International Symposium on Novel Aromatic Compounds (ISNA-14), Eugene, OR, USA, 24–29 July 2011.

‡Corresponding author: E-mail: yuming@mun.ca

The unique structural and redox properties of TTF have made it widely applicable in modern materials science, ranging from molecular electronics [3–7], photonics [8,9], magnetic materials [10,11], and photovoltaics [12–15], just to name a few. Over the past few decades, a major trend in TTF research has been centered on the development of efficient and scalable synthetic methodologies for preparing novel TTF derivatives with enhanced and/or unprecedented molecular properties as well as improved processability beneficial to device fabrication. Within this context, a vast array of TTF analogues has been synthesized and thoroughly characterized. Some prominent examples include TTF conductors/superconductors with high dimensionality [16,17], TTF macrocycles [18–20], and TTF polymers and dendrimers [21–23]. Moreover, as the synthetic toolbox continues to grow, TTF derivatives as a class of fascinating functional molecular building components have found increasing applicability in making molecular switches, shuttles, tweezers, and chemosensors to incorporate desirable redox and structural properties into these functional molecular devices [24–31].

A commonly used strategy for the design of new TTF derivatives is to expand the backbone of TTF through diverse π-spacers, leading to the so-called π-extended TTFs (exTTFs). Shown in Fig. 2 are a series of prominent representatives of exTTFs [32–39], among which the vinylogous and quinoid-type exTTFs (**2** and **3**) have attracted considerable interest in recent years, owing to their relatively low oxidation potentials. It is also worth mentioning that besides vinyl and aryl bridges, the structure of TTF

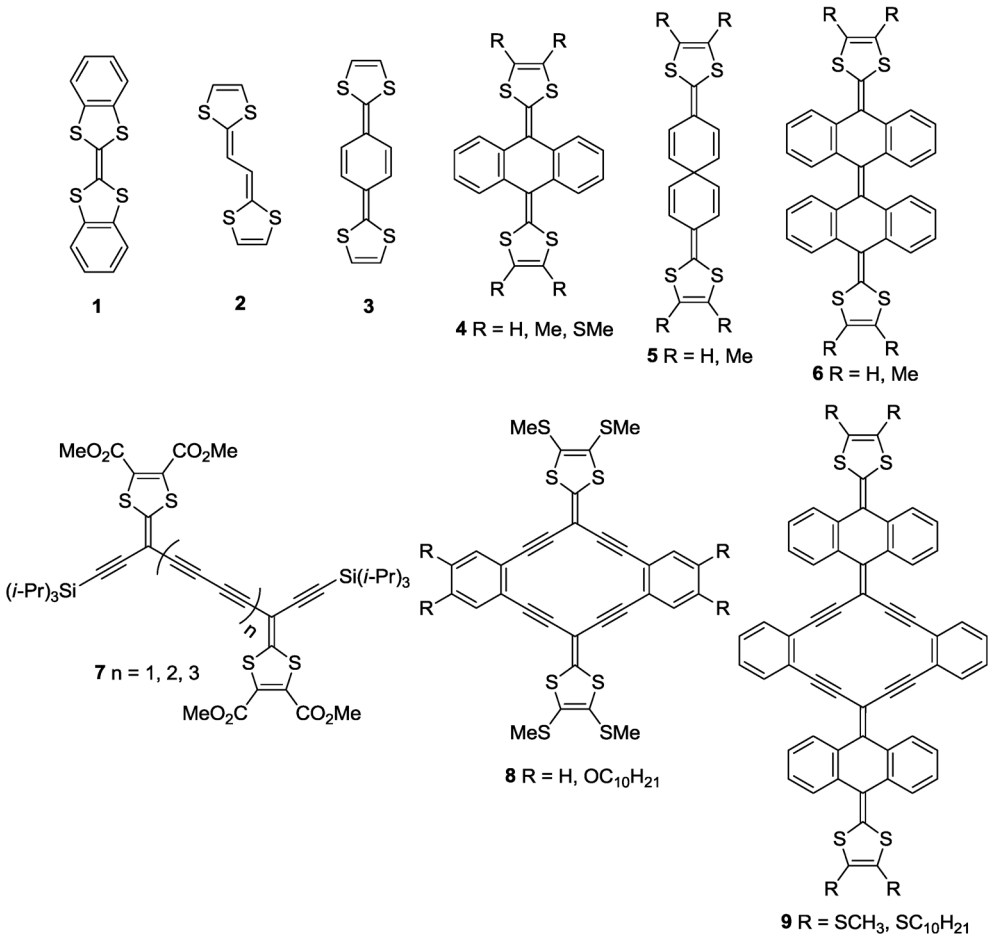

Fig. 2 Representatives of π-extended TTF analogues.

can be further expanded by insertion of acetylenic bonds to generate some highly π-extended TTF analogues. The marriage of TTF and acetylene chemistry brings about certain advantages in terms of material design and synthesis. The linear-shaped acetylenic unit facilitates intuitive and rational design of macromolecular systems possessing regular and predictable molecular shapes (e.g., shape-persistent macrocycles) and intermolecular organization. In addition, the facile chemistry arising from the alkynyl group, such as metal-catalyzed cross-coupling, homocoupling, and cycloaddition reactions, offers convenient modular synthetic approaches by which chemical functionalization, structural tailoring, and further expansion (e.g., cross-linking) can be flexibly carried out to make new hybrid materials.

In the past three years, diphenyl-substituted TTF vinylogues (TTFVs) have captured our attention as appealing molecular building blocks owing to their versatile redox and structural switchability and tunability. Unlike unsubstituted TTFV **2**, which assumes a planar molecular shape, diphenyl-substituted TTFV analogues usually adopt a highly twisted molecular structure in the ground state, with the two dithiole groups presenting a *pseudo-cisoid* conformation, as a result of the steric hindrance of the two phenyl substituents. When the phenyl group is unsubstituted or *para*-substituted, diphenyl-TTFV undergoes a simultaneous two-electron transfer to form stable dications (this has been termed the "potential inversion scenario"). The strong electrostatic repulsion between the two dithiolium rings thus forces the molecules to re-orient into a *trans* conformation, wherein the dithiolium rings are coplanar and the two phenyl moieties are sited nearly perpendicular to the plane of the two dithiolium rings. Figure 3 illustrates the bi-state conformational switching properties of a simple diphenyl-TTFV **10** based on density functional theory (DFT) calculations. The calculated molecular geometry of **10** and [$\mathbf{10}^{2+}$] are in good agreement with the X-ray crystallographic data of other diphenyl-substituted TTFV derivatives [40,41].

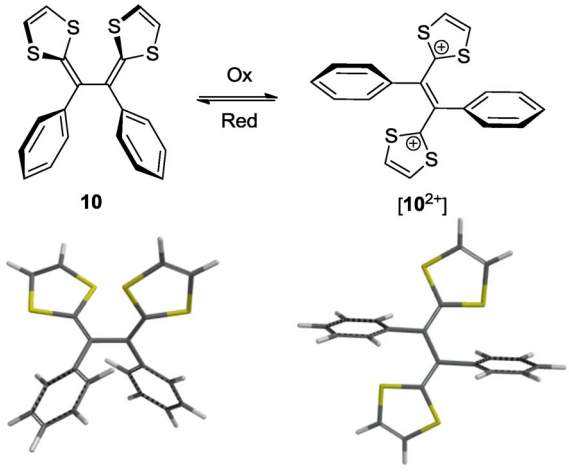

Fig. 3 Redox-controlled conformational switching behavior of diphenyl-TTFV **10**. The molecular geometries shown in the bottom were optimized at the B3LYP/6-311G* level of theory.

Our theoretical investigations also reveal that the electronic properties of diphenyl-TTFV derivatives are subject to the electronic nature of substituents. Figure 4 shows the linear correlation of the energies of highest occupied molecular orbital (HOMO) and lowest unoccupied molecular orbital (LUMO) with the substituent constant of *para*-substituted R group. The significant electronic substitution effect manifests a good tunability of electronic and redox properties of diphenyl-TTFVs at the molecular level, which in turn paves a way for design and synthesis of novel molecular materials with controllable electronic and optoelectronic properties and functions.

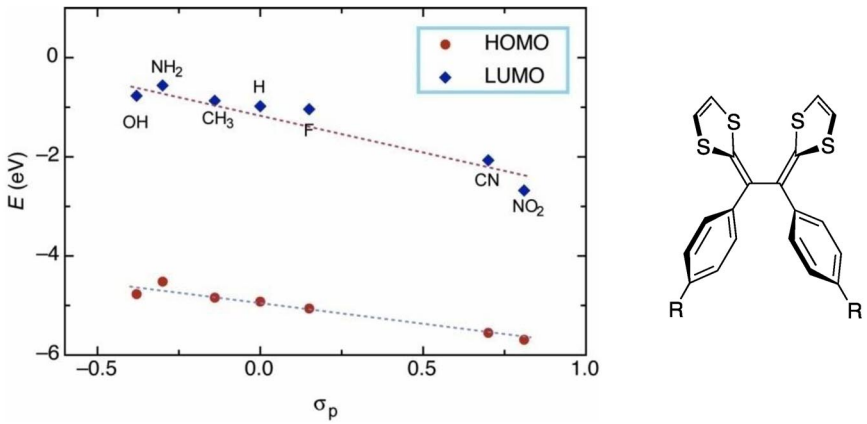

Fig. 4 Linear correlations between HOMO and LUMO energies of diphenyl-TTFV with the Hammett value (σ_p) of endgroup attached to the phenyl ring.

This article outlines our recent exploration of diphenyl-substituted TTFV as a *structural* and *functional* component for a series of novel carbon-rich π-conjugated molecular materials. So far, our studies have demonstrated that diphenyl-TTFV in conjunction with acetylenic scaffolding provides synthetic entry into π-conjugated polymers, shape-persistent macrocycles, functional chromophores/fluorophores, and electroactive donor/acceptor ensembles. Detailed property characterizations have suggested potential application in the fields of electrochromism, molecular switching devices, and chemical and biological sensors.

SYNTHESIS OF PHENYL-SUBSTITUTED DTF PRECURSOR

The synthesis of TTFV requires both C–C and C=C bond formation. For the olefination process, the Wittig, Horner–Wadsworth–Emmons (HWE), and McMurry coupling reactions have been employed in the preparation of a number of vinylogous TTFs [33,42–44]. In addition to these methods, an interesting approach involving base-promoted ring opening of 1,2,3-dithiadiazoles was devised by Becher and co-worker to generate TTFV structures [45]. Unfortunately, this method is very limited in producing substituted TTFVs. For diaryl-substituted TTFVs such as **10**, the most commonly used synthetic route is via the oxidative dimerization of corresponding dithiafulvene (DTF) precursors. The reaction mechanism of this dimerization was elucidated by Lorcy, Hapiot, and co-workers [46,47], and the detailed reaction steps are shown in Scheme 1. Treatment of an aryl-substituted DTF under oxidative conditions leads to the formation of DTF radical cation, which dimerizes to form a new C–C bond, yielding a diprotonated TTFV product. The dimerized product then undergoes proton loss to form neutral TTFV. Under oxidative conditions, the neutral TTFV is quickly converted into stable TTFV dication. When the oxidative dimerization is complete, a reduction reaction follows to reduce TTFV dication into neutral TTFV.

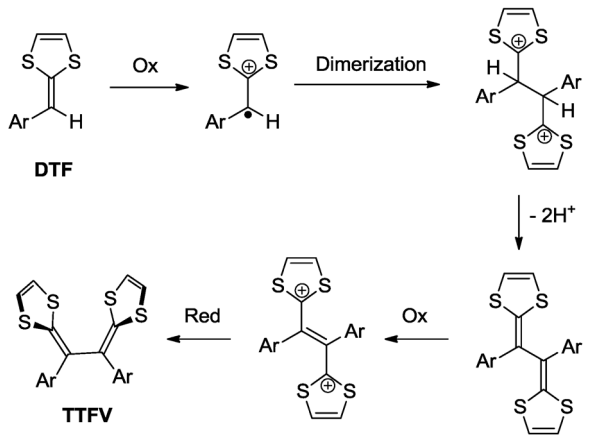

Scheme 1 Mechanism for oxidative dimerization of aryl-DTF to form diaryl-TTFV.

A variety of oxidants has been reported to promote this type of dimerization reaction, including I_2, $(BrC_6H_4)_3SbCl_6$, $AgBF_4$, and Br_2 [40,48–56]. Their efficiency in promoting the dimerization varies, depending on the structure of DTF precursor, while in most cases I_2 and $AgBF_4$ gave satisfactory results. Based on this facile synthetic methodology, we have prepared a group of diphenyl-TTFVs with acetylenic groups substituted at the *para*-position of the phenyl moiety. In the synthesis, acetylenic-DTF precursors need to be prepared beforehand. Scheme 2 outlines the synthetic route to a trimethylsilylacetylene (TMSA) substituted DTF precursor **13a** via an HWE olefination approach. Phosphonate **11** was deprotonated with *n*-BuLi at low temperature to form an ylide in situ, which subsequently reacted with alkynyl benzaldehyde **12** to afford DTF **13a** in good yield.

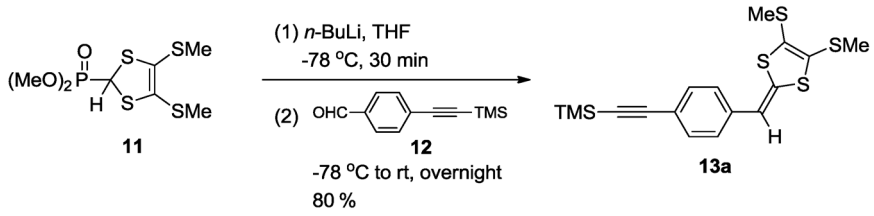

Scheme 2 Synthesis of DTF **13a** via HWE reaction.

A bottleneck in the preparation of **13a** is the synthesis of the precursor phosphonate **11**. The conventional preparation protocol follows a multi-step synthetic route shown in Scheme 3 [57]. This approach involves both tedious purification steps and the use of costly reagents (e.g., HBF_4), which hinders the large-scale production of **11** in an economical and concise manner.

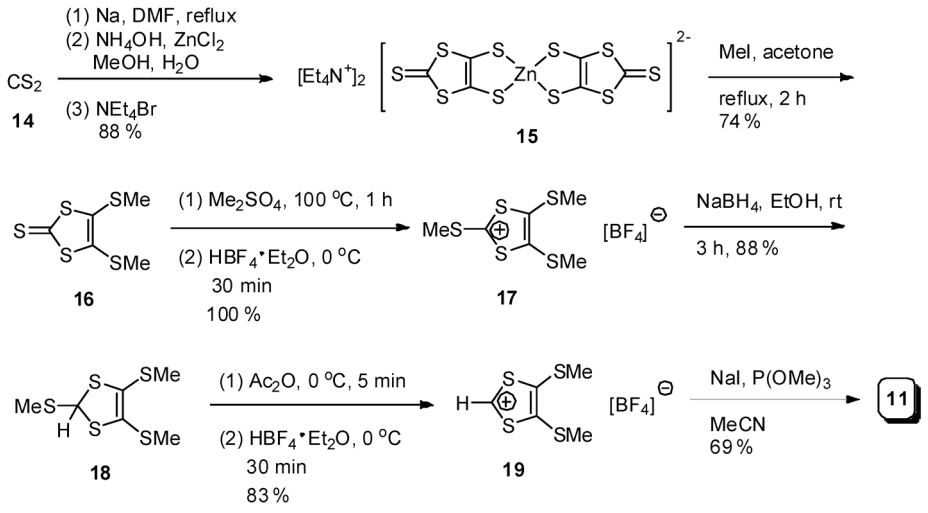

Scheme 3 Multi-step synthesis of phosphonate precursor **11**.

To circumvent such a lengthy synthetic route, an alternative approach based on a phosphite-mediated olefination method devised by Bryce and co-workers [58] was then explored. As shown in Scheme 4, thione **16** was directly cross-coupled with aldehyde **12** in the presence of a large excess of $P(OMe)_3$ to afford DTF **13a**. This reaction proceeded smoothly in toluene at 100 °C to give **13a** in a yield of 64 %. Compared with the previous HWE reaction method, this one-step route features a significant improvement. Nevertheless, it still does not provide a satisfactory solution to large-scale synthesis, because lengthy column chromatographic separation of **13a** from unreacted $P(OMe)_3$ must be conducted after the reaction. Development of purification methods that are both labor- and cost-effective is currently under investigation.

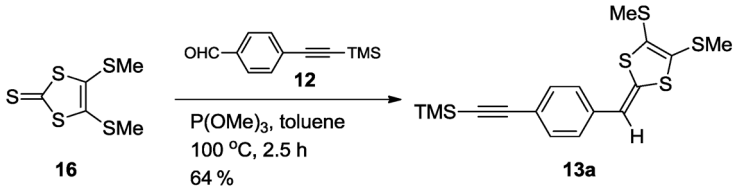

Scheme 4 Synthesis of DTF **13a** through a $P(OMe)_3$-promoted olefination reaction.

SYNTHESIS AND PROPERTIES OF OLIGOYNE-CENTERED TTF ANALOGUES AND RELATED POLYMERS

With acetylenic DTF **13a** in hand, a series of oligoyne-centered exTTF derivatives was synthesized through the procedures depicted in Scheme 5 [59,60]. Desilylation of DTF **13a** with K_2CO_3 gave a free terminal alkyne intermediate which was immediately subjected to a Hay coupling reaction under the catalysis of CuI/TMEDA to afford diyne-exTTF **20a** in 60 % yield. Mono-alkynylated DTF **13a** after desilylation could also be coupled with excess TMSA under Hay coupling conditions to yield diyne-DTF **13b** in 82 % yield. Compound **13b** was desilylated and coupled with TMSA under the catalysis of CuI/TMEDA, giving triyne-DTF **13c** in 60 % yield. By the same token, diyne and triyne **13b,c** were subjected to the desilylation/coupling sequence, giving tetrayne-exTTF **20b** and hexayne-exTTF **20c** in high yields. It is worth noting that that diyne and tetrayne **20a,b** are stable orange-colored solids,

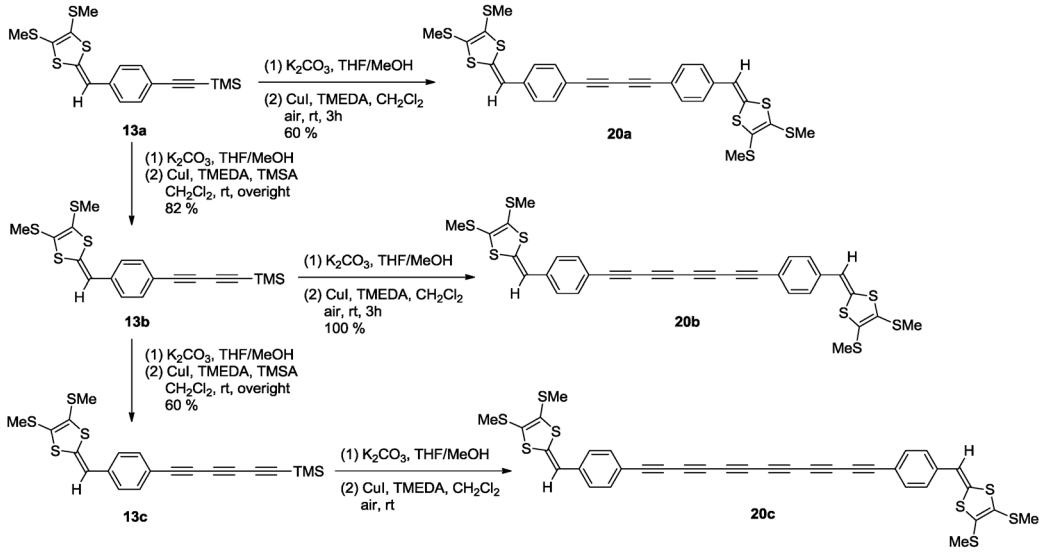

Scheme 5 Synthesis of oligoyne-DTFs **13** and oligoyne-centered exTTFs **20** via Cu(I)-catalyzed alkynyl coupling reactions.

whereas hexayne **20c** only retains stability in dilute solution. Evaporation of the solution of **20c** led to the formation of a dark purple solid that is insoluble in any solvents. The poor chemical stability of **20c** in the solid state is attributed to the topochemical polymerization of π-conjugated hexayne units.

The solid-state structural properties of diyne-exTTF **20a** and tetrayne-exTTF **20b** were investigated by single-crystal X-ray diffraction analysis. Figure 5 shows the molecular geometries and crystal packing of **20a,b**. Both compounds assume a nearly planar conformation in which the two exterior DTF rings are slightly deviated from the molecular plane by 15–20º (see Fig. 5A,B). In the crystal lattice of **20a**, the molecules are aligned in a parallel fashion where the distance between adjacent butadiyne moieties (d) is 5.35 Å and the inclination angle (ϕ) is 57.2º. For tetrayne **20b**, the packing parameters are $d = 5.34$ Å and $\phi = 48.8$º, which suggests that **20b** has a stronger tendency towards topochemically controlled polymerization than diyne **20a**. The solid-state reactivity of **20a,b** for polymerization is also manifested by thermal analysis. Differential scanning calorimetric (DSC) analysis shows that tetrayne **20b** undergoes a prominent exothermic process ($\Delta H = -249.7$ kJ mol^{-1}) at 226.9 °C, while for diyne **20a** an exothermic process takes place at higher temperature and with relatively smaller reaction heat (244.5 °C, $\Delta H = -171.4$ kJ mol^{-1}).

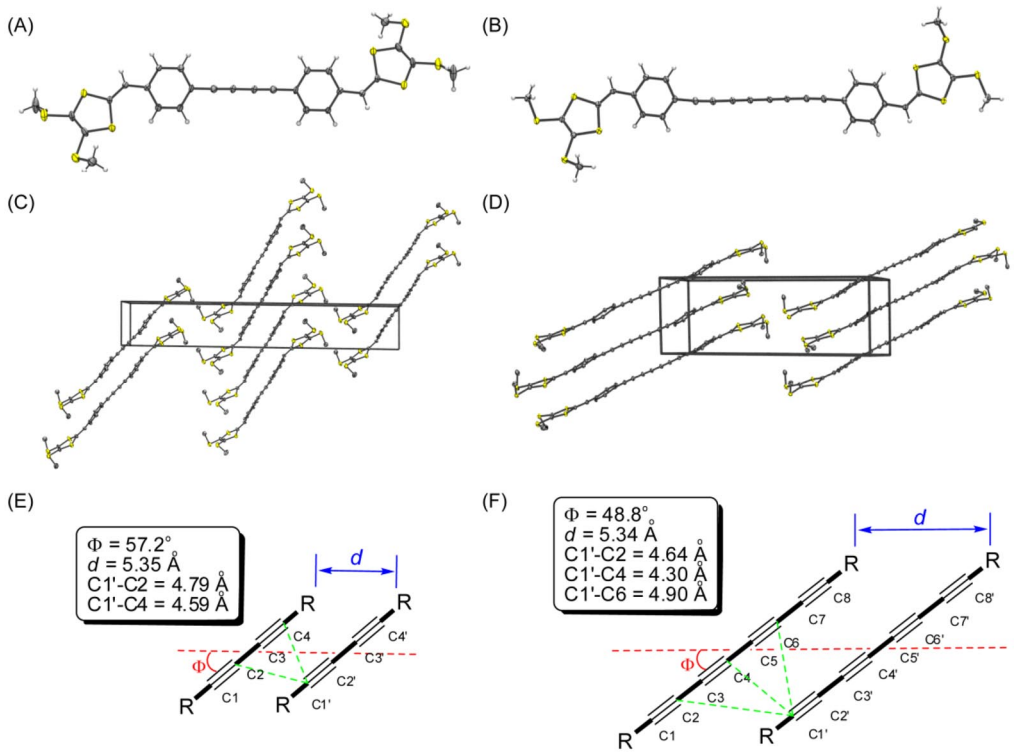

Fig. 5 (A) ORTEP drawing of diyne-exTTF **20a** (30 % probability thermal ellipsoids). (B) ORTEP drawing of diyne-exTTF **20b** (30 % probability thermal ellipsoids). (C) Crystal packing of **20a** viewed perpendicular to the *b*-axis. (D) Crystal packing of **20b** viewed perpendicular to the *b*-axis. (E) Packing geometry of **20a** in the solid state. (F) Packing geometry of **20b** in the solid state.

The electronic absorption properties of oligoyne-exTTFs **20a–c** were investigated by UV–vis spectroscopy and representative spectral data are given in Fig. 6. In the spectrum of diyne **20a**, a low-energy absorption band emerges at 423 nm, which is assigned to π–π* electronic transition. For tetrayne **20b**, this low-energy transition is red-shifted by ca. 40 nm as a result of increased π-conjugation. The

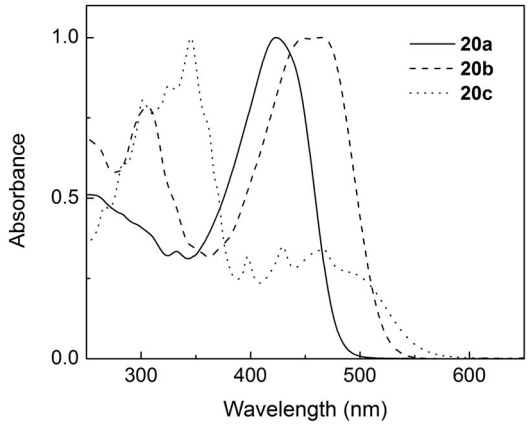

Fig. 6 Normalized UV–vis spectra for oligoyne-centered exTTFs **20a–c** measured in $CHCl_3$.

spectrum of hexayne **20c** shows distinctive vibrational progressions, the spacings of which are consistent with those reported for analogous hexaynes or higher oligoynes in the literature [61].

The electrochemical properties of oligoyne-exTTFs **20a,b** were studied by cyclic voltammetry. The cyclic voltammograms of diyne **20a** and tetrayne **20b** show continuous growth of a redox couple that is characteristic of the TTFV unit. This observation indicates that the DTF moieties of **20a,b** can undergo oxidative coupling reactions under electrochemical conditions to form conducting polymers on the surface of the working electrode. Indeed, it was found that multiple cyclic voltammetric scans or bulk electrolysis led to the formation of high-quality and robust polymer thin films on conductive substrates. Figures 7C,D show the cyclic voltammograms of thin films of poly[**20a**] and poly[**20b**] electrochemically deposited on indium tin oxide (ITO)-coated glass slides. Both polymer films exhibit a quasi-reversible redox wave pair, while the formal potentials, $E^\circ = (E_{pc} + E_{pa})/2$, are similar to that of the TTFV monomer, indicating that the TTFV units in the polymers dictate the electrochemical activity.

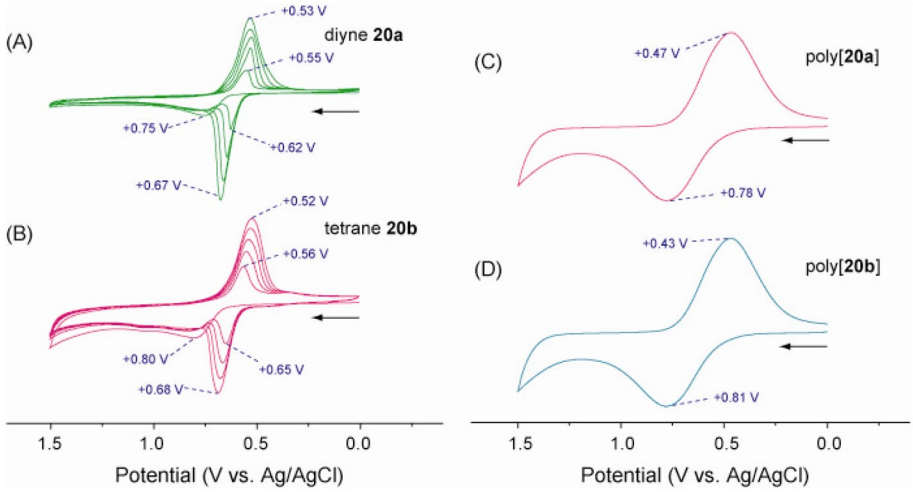

Fig. 7 Cyclic voltammograms of (A) diyne-exTTF **20a**, scan rate: 200 mV s^{-1}, working electrode: glassy carbon; (B) tetrayne-exTTF **20b**, scan rate: 200 mV s^{-1}, working electrode: glassy carbon; (C) poly[**20a**] thin film, scan rate: 50 mV s^{-1}, working electrode: ITO glass; (F) poly[**20b**] thin film, scan rate: 50 mV s^{-1}, working electrode: ITO glass. Experimental conditions: supporting electrolyte: Bu_4NBF_4 (0.1 M); solvent: CH_2Cl_2; counter electrode: Pt; reference electrode: Ag/AgCl. The arrows indicate the initial potential scan direction.

The electrodeposited polymer thin films of poly[**20a**] and poly[**20b**] on ITO glass exhibit electrochromic properties. In the neutral state, poly[**20a**] is pale yellow in color and its UV–vis absorption spectrum gives an absorption band at 441 nm and a weak absorption tail ranging from 500 to 700 nm (see Fig. 8A). After electrolysis of the film at +0.9 V (vs. Ag/AgCl) for 1 min, the color of the polymer thin film turns to dark green and a new broad absorption band from 500 to 850 nm emerges in the vis–NIR region, which is attributed to the formation of $[TTFV]^{2+}$. The resulting cationic polymer thin film can be then reduced to the neutral state after electrolysis at –0.3 V (vs. Ag/AgCl) for 0.5 min to change the color back to pale yellow. The coloration and de-coloration processes can be reversibly switched by altering the electrode potential, suggesting application in electrochromic devices. Similar electrochromic effects can be observed for the thin film of poly[**20b**] as well (see Fig. 8B). Of particular note is that the UV–vis spectrum of cationic poly[**20b**] shows vibrational fine structures of the tetrayne moiety, indicating that the oligoyne units remain intact during the oxidation process.

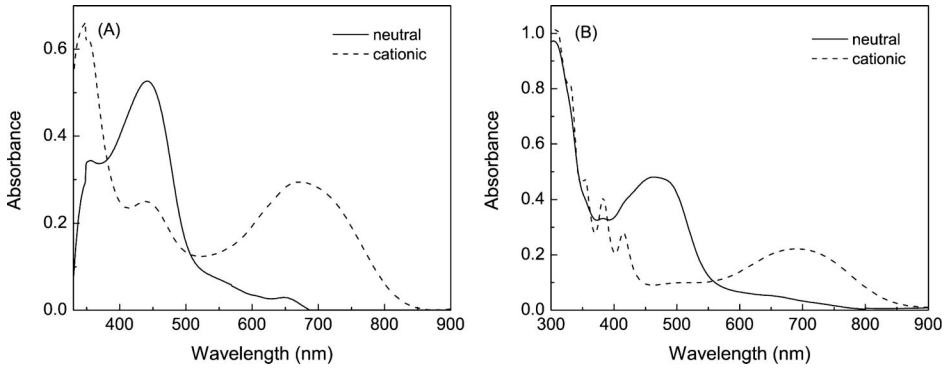

Fig. 8 (A) UV-vis absorption spectra of poly[**20a**] on ITO glass in the neutral (solid line) and cationic (dashed line) states. (B) UV–vis absorption spectra of poly[**20b**] on ITO glass in the neutral (solid line) and cationic (dashed line) states.

In addition to electrochemical polymerization, the preparation of TTFV-oligoyne polymers via chemically induced oxidative coupling reactions was also investigated. As shown in Scheme 6, diyne **20a** and tetrayne **20b** were treated with I_2 in CH_2Cl_2 at room temperature for 12 h. After reductive work-up with aq. $Na_2S_2O_3$, polymeric products were obtained as orange-colored solids that are soluble in nonpolar organic solvents. However, these products do not have high degrees of polymerization. Instead, they are rather short oligomers, ranging from dimer to octamer for poly[**20a**] and dimer to tetramer for poly[**20b**], as evidenced by matrix-assisted laser desorption/ionization with time-of-flight mass spectrometry (MALDI-TOF MS) analysis.

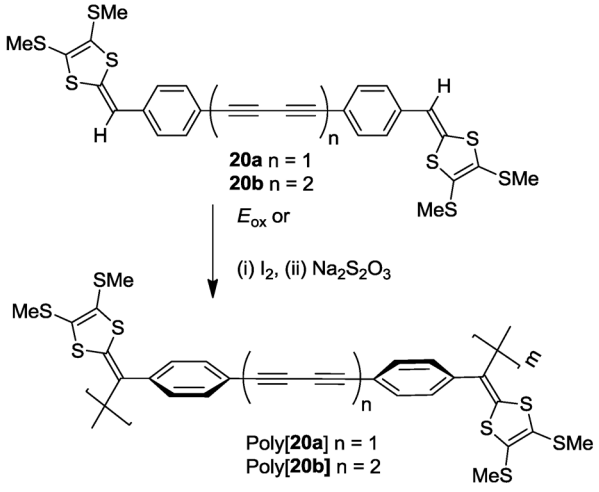

Scheme 6 Synthesis of TTFV-oligoyne polymers by oxidative coupling reaction.

SYNTHESIS AND PROPERTIES OF TTFV-BASED SHAPE-PERSISTENT MACROCYCLES

Acetylenic DTFs **13a,b** were subjected to an iodine-promoted oxidative dimerization followed by $Na_2S_2O_3$ reduction to give TTFV derivatives **21a,b** in reasonable yields (Scheme 7) [59,60]. TTFVs **21a,b** were then desilylated to afford free terminal alkyne products. In our initial studies, desilyated **21a**

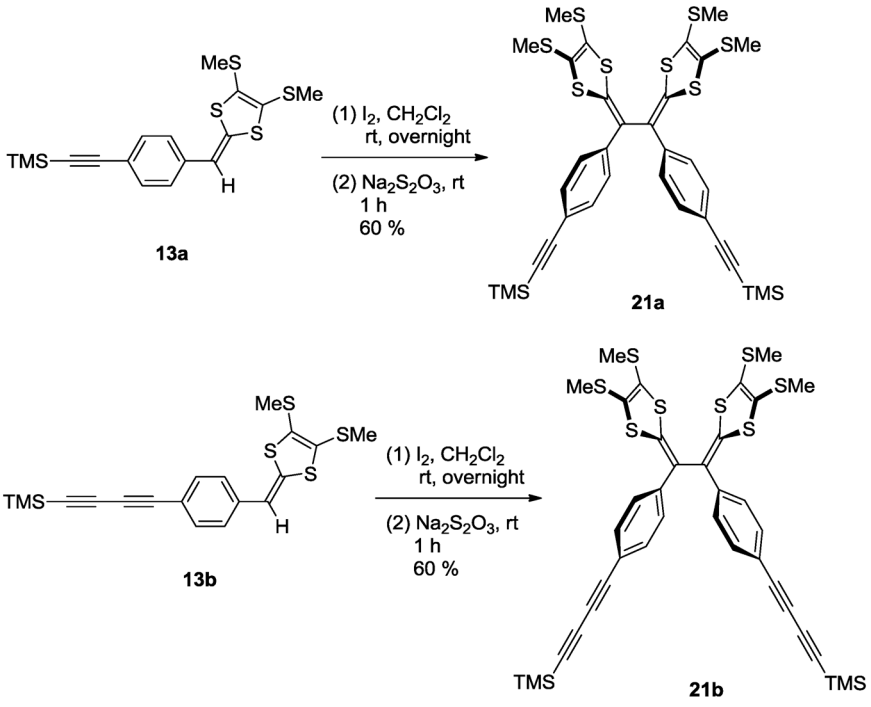

Scheme 7 Synthesis of acetylenic TTFVs **21a,b** via oxidative dimerization.

was subjected to a Cu(I)-catalyzed alkynyl homocoupling reaction with the hope to obtain polymer products similar to those acquired via the electrochemical polymerization as outlined in Scheme 6. To our surprise, the homocoupling reaction ended with a complex mixture of oligomers, while MALDI-TOF MS analysis revealed the formation of a series of cyclic oligomers (trimer to pentamer) rather than chain-like polymers. This result was somewhat counterintuitive at first glance, considering the non-planar molecular shape of **21a** indicated by X-ray crystal structure analysis (Fig. 9). Nevertheless, cyclic molecular frameworks containing TTFV units were not unprecedented prior to our work. Lorcy and co-workers reported the formation of TTFV tetrameric and pentameric macrocycles resulting from electrolysis of a phenyl-DTF precursor [62].

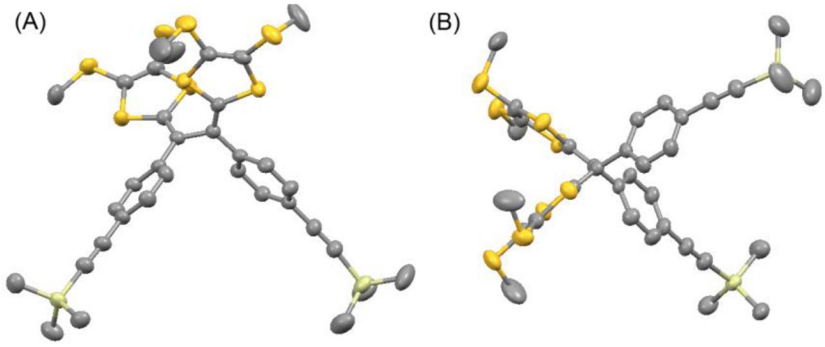

Fig. 9 X-ray single-crystal structure of compound **21a**: (A) front view; (B) side view (CCDC 845793).

The Cu(I)-catalyzed homocoupling reaction afforded macrocyclic products only in trace amounts. To further improve the efficiency of the reaction, a number of catalytic conditions have been explored. Eventually, a Pd(II)/Cu(I) co-catalyst system similar to that reported by Iyoda and co-workers [63] in their synthesis of TTF-[18]annulenes was found to give the best outcome. As shown in Scheme 8, a one-pot macrocyclization of desilyated **21a** under Pd/Cu/TMEDA catalysis afforded shape-persistent macrocycle **22a** in 18 % yield. In a similar manner, shaped macrocycle **22b** was made from homocoupling of **21b**; however, purification of **22b** encountered tremendous difficulty owing to the presence of some intractable oligomer byproducts.

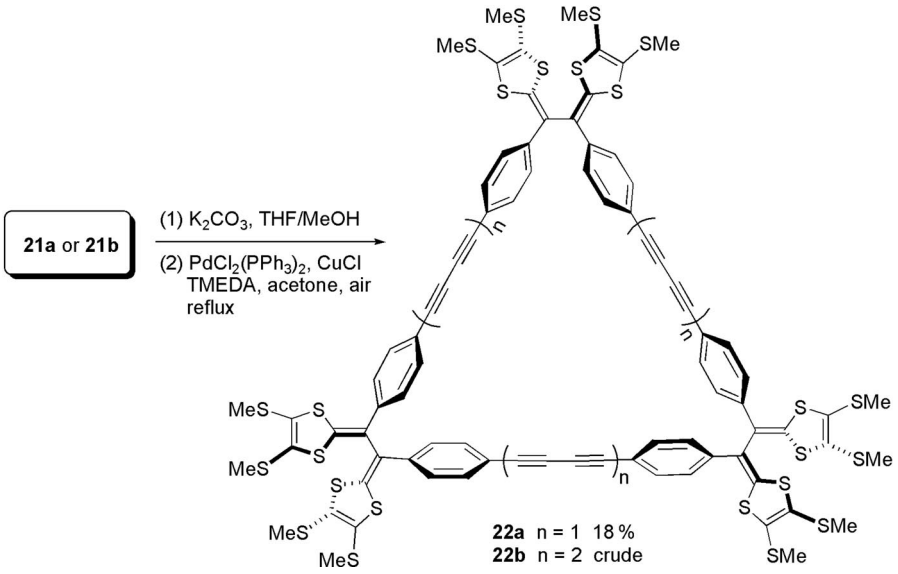

Scheme 8 Synthesis of shape-persistent TTFV macrocycles **22a**,**b** via Pd/Cu-catalyzed homocoupling macrocyclization.

The structural properties of trimeric macrocycle **22a** were investigated by semi-empirical calculations using a reparameterized AM1 method (RM1). In the optimized molecular geometry of **22a**, the TTFV unit exhibits only a small degree of twisting compared with that of monomer **21a**. The strain energy arising from macrocyclization is calculated to be 7.48 kcal mol^{-1} [60], which is certainly an affordable energy cost for the cyclization reaction. The low strain energy of **22a** accounts for its preferential formation over other cyclic oligomer products such as tetramer and pentamer. MALDI-TOF MS confirmed the formation of such higher macrocycles during the macrocyclization reaction; however, they were formed only in trace amounts.

The electrochemical redox behavior of macrocycle **22a** was studied by cyclic voltammetry. Macrocycle **22a** gives a pair of quasi-reversible redox waves at E_{pa} = +0.82 V and E_{pc} = +0.56 V in its cyclic voltammogram. In comparison with the cyclic voltammogram of monomeric TTFV **21a**, the redox potentials of **22a** is shifted anodically by ca. 0.1 V. The shift is attributed to the constrained *cis*-conformation of TTFV in the macrocycle skeleton. Similar conformational effects on redox behavior of TTFV were also observed in poly(ethylene glycol) tethered TTFV macrocycles reported by Lorcy and co-workers [64].

SYNTHESIS AND PROPERTIES OF TTFV-BASED MOLECULAR TWEEZERS

The V-shaped molecular structure of acetylenic TTFV **21a** serves as a versatile structural element for construction of functional molecular hybrids via various metal-catalyzed alkynyl coupling reactions. With this objective in mind, we have explored the synthesis of a group of TTFV-centered tweezer-like compounds [65]. As shown in Scheme 9, desilylation of TTFV **21a** with K_2CO_3 followed by Sonogashira cross-coupling with 2-iodoanthraquinone (**23**) afforded compound **24** in 66 % yield. Given the electron-donating properties of TTFV and the electron-accepting nature of anthraquinone (AQ), compound **24** can be viewed as an acceptor–donor–acceptor triad.

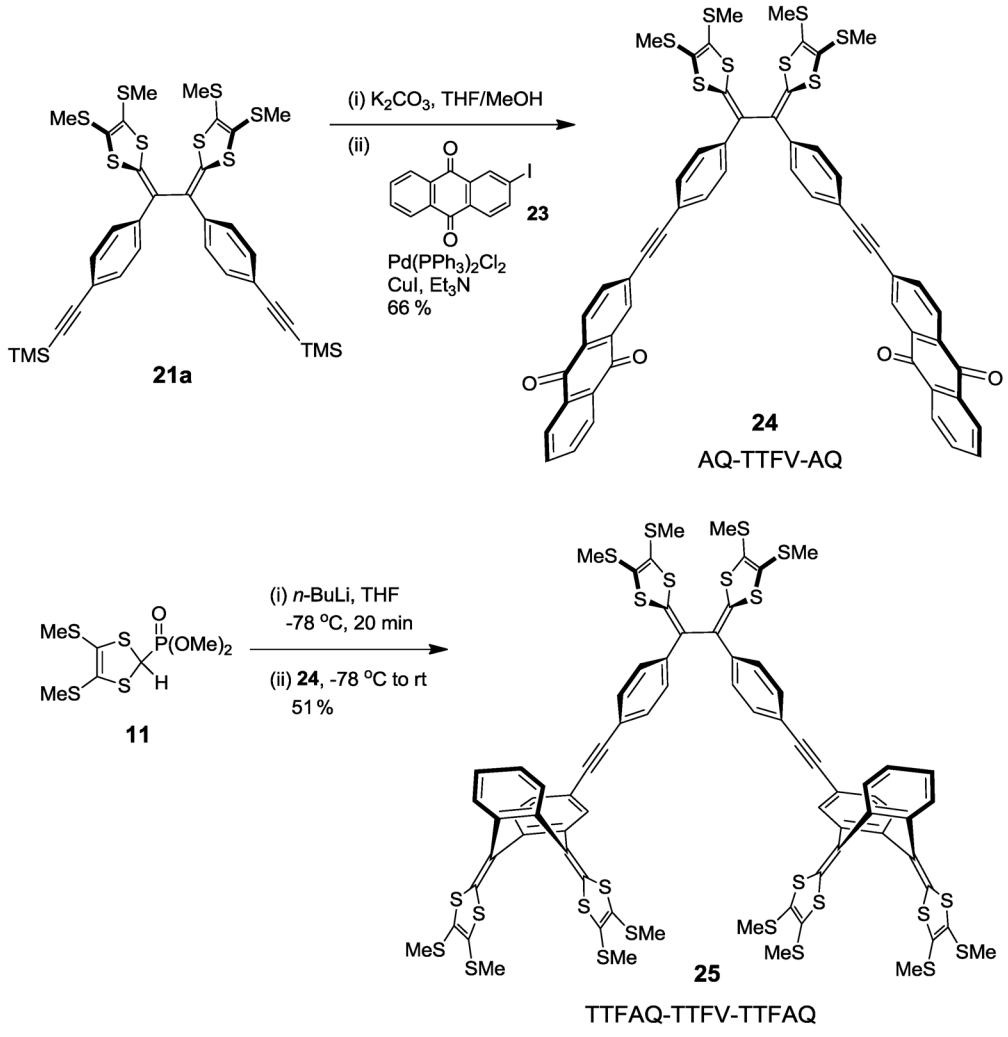

Scheme 9 Synthesis of TTFV-hinged molecular tweezers **24** and **25** as functional donor/acceptor triads.

AQ-TTFV-AQ **24** could undergo a two-fold HWE reaction with the ylide in situ generated from treatment of phosphonate **11** with *n*-BuLi. The reaction proceeded at low temperature, affording compound **25** in 51 % yield. Note that the olefination reaction converted the two electron-withdrawing AQ moieties into two electron-donating anthraquinoid-type π-extended tetrathiafulvalene (TTFAQ) groups, hence rendering **25** a donor–donor–donor triad.

The redox properties of TTFV tweezers **24** and **25** are revealed by their cyclic voltammograms shown in Fig. 10A. AQ-TTFV-AQ **24** displays a pair of reversible redox waves at E_{pa} = +0.61 V and E_{pc} = +0.54 V in the positive potential window, which is assigned to the two-electron transfer of TTFV. The formal potential of this redox wave pair is slightly greater than that of TTFV **21a**, indicating weak electronic communication between the AQ and TTFV units. In the negative potential region, two redox wave pairs are observed and ascribed to the successive electron transfer on the two AQ moieties. The cyclic voltammogram of TTFAQ-TTFV-TTFAQ **25** shows one oxidation peak at +0.68 V in the anodic scan, which is ascribed to a simultaneous 6-electron transfer at the two TTFAQ and one TTFV units. In the cathodic scan, two reduction peaks are seen at +0.55 and +0.23 V, respectively. The origins of these peaks are assigned to successive reductions of TTFAQ and TTFV units.

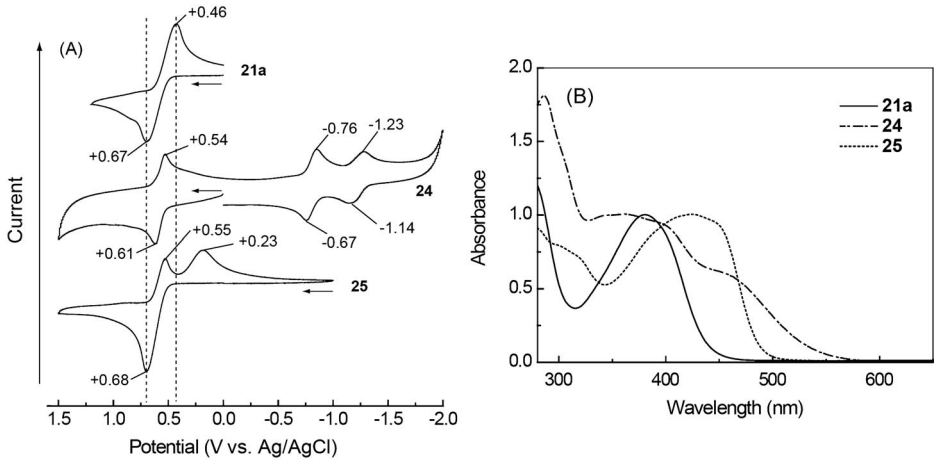

Fig. 10 (A) Cyclic voltammograms of TTFV derivatives **21a**, **24**, and **25**. Experimental conditions: analyte (ca. 10^{-3} M); Bu_4NBF_4 (0.1 M) as supporting electrolyte; CH_2Cl_2 as solvent; glassy carbon as working electrode; Pt wire as counter electrode; Ag/AgCl as reference; scan rate 0.1 V s^{-1}. (B) UV–vis spectra of **21a**, **24**, and **25** measured in CH_2Cl_2.

The electronic absorption properties of TTFV derivatives **21a**, **24**, and **25** are compared in Fig. 10B. Acceptor–donor–acceptor triad **24** shows a notable long-wavelength absorption shoulder at 460 nm as well as a broad absorption tail extending to 580 nm. The spectral features indicate a significant degree of intramolecular charge transfer between donor (TTFV) and acceptor (AQ) units via the acetylenic linkages in triad **24**.

The capability of tweezer-like TTFV triads **24** and **25** in forming supramolecular complexes with some aromatic species, including nitrobenzene, [60]fullerene, and [6,6]-phenyl-C_{61}-butyric acid methyl ester (PCBM), was assessed in various organic solvents. Unfortunately, none of the compounds exhibited strong binding with the two molecular tweezers. It is reasoned that the rigidity of acetylenic linkers does not facilitate a cooperative binding mode. Further structural tailoring of the linkage group is therefore necessary if supramolecular binding and recognition functions are desired for TTFV molecular tweezers.

The acetylenic groups in TTFV **21a** allow the popular "click" chemistry to be implemented to access a wide spectrum of functional TTFV hybrids by a rapid and modular approach. The "click" synthetic strategy has such advantages as high yielding, easy purification, mild reaction conditions, and good tolerance to various functionalities. So far, the most widely used click reaction is the Cu(I)-catalyzed alkyne-azide cycloaddition (CuAAC) reaction [66,67]. It is worth noting that numerous recent publications have demonstrated that the product of CuAAC reaction, 1,2,3-triazole, not only serves as

a robust linker group for building up complex molecular structures [68], but can act as an efficient ligand to bind with various metal ions [69–76], anions [77–80], and biomolecules [81,82]. In this sense, CuAAC-based "click" functionalization can be a synthetically economical way for constructing molecular and supramolecular systems with special ligand or receptor functions. In our recent work, TTFV derivatives "click" functionalized with chromophore or synthetic receptor groups have been sought. As shown in Scheme 10, TTFV **21a** was first desilylated by tetrabutylammonium fluoride (TBAF) to afford free alkyne **26**. Compound **26** was reacted with azido-anthracene **27** in the presence of CuI and diisopropylethylamine (DIPEA) to give dianthryl-TTFV **28** in 91 % yield.

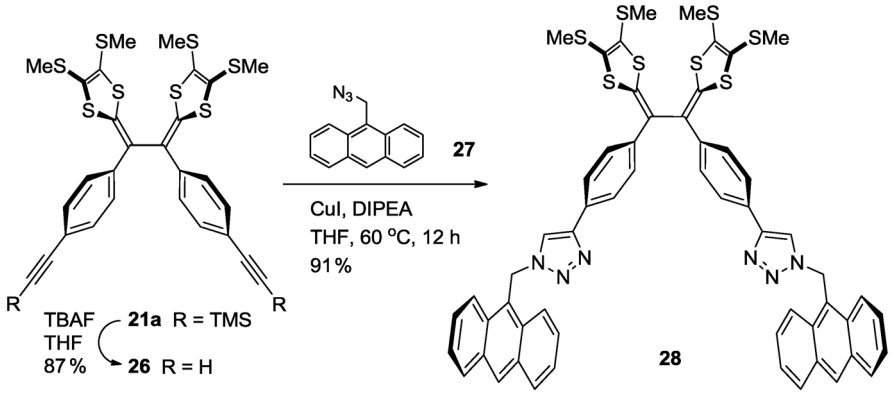

Scheme 10 Synthesis of dianthryl-TTFV **28** by click reaction.

Although containing two fluorogenic units (anthracene), compound **28** showed very weak fluorescence [$\Phi = 0.009$ in tetrahydrofuran (THF)]. The quenched emission is due to the photoinduced electron transfer (PET) [83] from donor (TTFV) to acceptor (anthracene) units. It was anticipated that when the triazole groups of compound **28** were bound to metal ions, the PET process would be attenuated to give rise to fluorescence enhancement. If such were the case, dianthryl-TTFV **28** would hence act as a fluorescence turn-on sensor for certain metal ions. To test this sensor design concept, dilute THF solution of **28** was subjected to fluorescence titration with a number of transition-metal ions, including Cu^{2+}, Fe^{2+}, Cd^{2+}, Mn^{2+}, Zn^{2+}, Hg^{2+}, Pb^{2+}, and Ag^{+}. For comparison, titration with a strong Brønsted acid, trifluoroacetic acid (TFA), was also conducted; however, protonation of **28** did not result in significant fluorescence enhancement. Of the eight metal ions tested, Cu^{2+}, Fe^{2+}, and Cd^{2+} gave rise to very significant fluorescence enhancement. Figure 11A illustrates the fluorescence spectral changes of **28** in titration with Cu^{2+}. At the endpoint of titration, the fluorescence intensity is increased by 26-fold at 415 nm (limit of detection: 0.26 μM). Note that the substantial fluorescence enhancement of **28** contrasts markedly the fluorescence quenching effect of Cu^{2+} ion on an anthryl-triazole sensor recently reported by Varazo et al. [84]. The TTFV donor is believed to play a pivotal role in effecting the fluorescence turn-on behavior.

Figure 11B gives the sensitivity of **28** toward a series of cations. Herein a decreasing trend is observed as follows: $Cu^{2+} > Fe^{2+} > Cd^{2+} > Ag^{+} > Mn^{2+} > Zn^{2+} \sim Hg^{2+} > Pb^{2+} > H^{+}$. To quantify the affinity of **28** for various metal ions, the fluorescence titration data were subjected to SPECFIT global analyses [85]. The analyses reveal that **28** can bind with transition-metal and proton cations to form both 1:1 and 1:2 complexes, while the binding constants vary substantially depending on the nature of metal ions. Plotting the binding constants ($\log\beta_{11}$ and $\log\beta_{12}$) against the standard electrode potentials of the metal ions (E°) gives interesting correlations. As shown in Fig. 12, the cations fall in two distinct groups in terms of linear relationship between $\log\beta$ and E°. Group I consists of Cu^{2+}, Cd^{2+}, Zn^{2+}, Fe^{2+}, and Mn^{2+} ions, which afford considerably larger binding constants than those of Group II, which

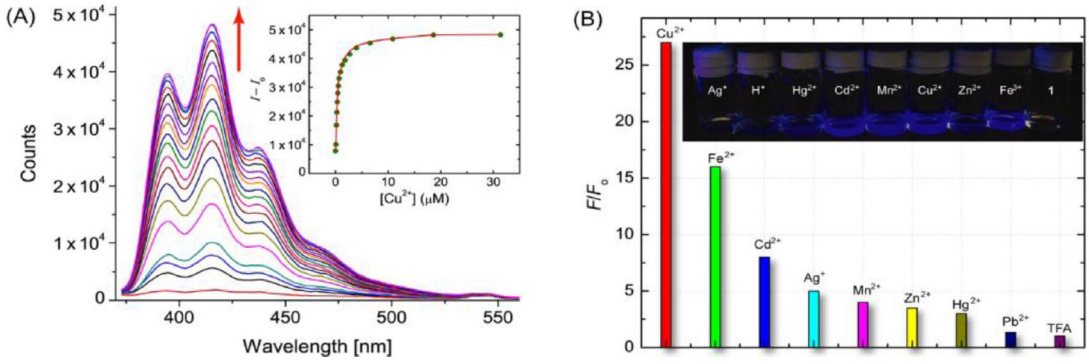

Fig. 11 (A) Fluorescence titration of **28** (5.55 μM) with $Cu(OTf)_2$ in THF (λ_{ex} = 350 nm). Inset: Stern–Volmer plot calculated from emission at λ = 415 nm. (B) Fluorescence enhancement (λ = 415 nm) at the endpoint of titration. Inset: photographic images of solutions of **28** with various transition-metal ions and TFA in THF under irradiation of a UV lamp.

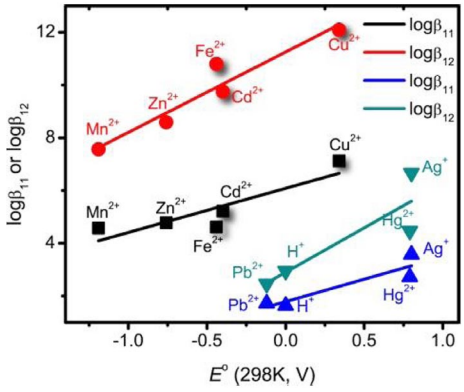

Fig. 12 Linear correlations of binding constants (logβ) and standard electrode potentials (E°) of transition-metal and proton cations.

includes Ag^+, Hg^{2+}, H^+, and Pb^{2+} ions. These observations are in line with expectations based on hard-soft acid/base (HSAB) theory. The three metal ions (Cu^{2+}, Fe^{2+}, and Cd^{2+}, highlighted by shadow in Fig. 12) that cause sizeable fluorescence enhancement of **28** have two common features: (1) they belong to Group I, and (2) their E° values match the low oxidation potential of TTFV to efficiently attenuate the PET process from TTFV to anthracene. Overall, the relationships disclosed in Fig. 12 are instructive for further design and fine-tuning of the selectivity and sensitivity of chemosensors in analogous molecular architectures.

Apart from fluorogenic groups, the diphenyl-TTFV core can also be functionalized with other types of ligands or receptors to attain chemical sensing properties. Scheme 11 depicts the synthesis of a TTFV-phenylboronic acid hybrid, compound **32**. By the CuAAC reaction, acetylenic TTFV **26** was coupled with azido-phenylboronate **29** to give compound **30** in 87 % yield. Compound **30** was then converted into trifluoroboronate **31** upon treatment with KHF_2. Hydrolysis of **31** in the presence of LiOH afforded TTFV-boronic acid **32** in a good yield.

Phenylboronic acid has been well known for its ability to effectively bind with saccharides in aqueous media [86–91]. If the binding of **32** to saccharides significantly influences the redox potentials of adjacent TTFV units, the binding event can be reported by electrochemical readouts detected by

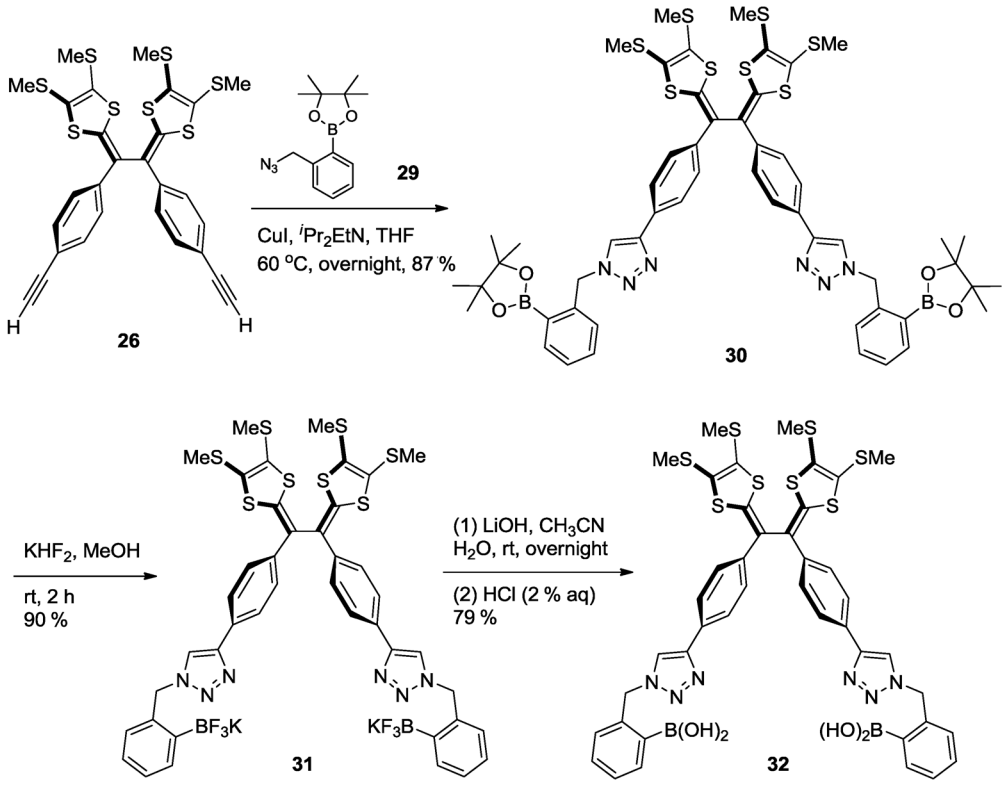

Scheme 11 Click synthesis of phenylboronic acid-TTFV hybrid **32**.

either potentiometric or voltammetric techniques. In this light, compound **32** was expected to show electrochemical sensing performance for saccharide molecules. To test the electrochemical sensing function, compound **32** was dissolved in aqueous phosphate buffer solution/DMSO (2:1) to maintain a neutral pH value (7.4) similar to that of physiological conditions, and to this solution various saccharides were titrated. The titration processes were monitored by differential pulse voltammetry (DPV).

Figure 13A depicts the DPV changes of TTFV boronic acid **32** in titration with fructose. It can be clearly seen that the current peak at +0.33 V increases steadily in intensity with increasing addition of fructose. It should be noted that the significant electrochemical responses were detected at mM concentrations of fructose and neutral pH, which is suggestive of effective binding between **32** and fructose under such conditions. In general, the binding of phenylboronic acid to *cis*-diol species is reversible in aqueous media, while only under basic conditions the equilibrium would favor the complexation product. Theoretical modeling studies suggest a "water-insertion" binding mode as shown in Fig. 13B, wherein the "click" generated triazole linker acts as an H-bond acceptor to facilitate the coordination of a water molecule with the boron atom [92]. Such a complexation mode is similar to that of the "Wulff-type" receptors [93–95] widely used for complexing with saccharides at neutral pH. It is therefore believed that the triazole group plays a key role in enhancing the binding of **32** with saccharides under physiological conditions. Similar DPV responses were observed in the titration experiments of compound **32** with ribose and galactose, indicating practical use of **32** as an electrochemical sensor for these saccharides. In the titration of glucose, however, the DPV profile of **32** was changed in a weak and random fashion, which is attributed to insignificant binding between glucose and compound **32**. Investigations into the exact binding modes, with which compound **32** binds to various saccharides, are currently underway.

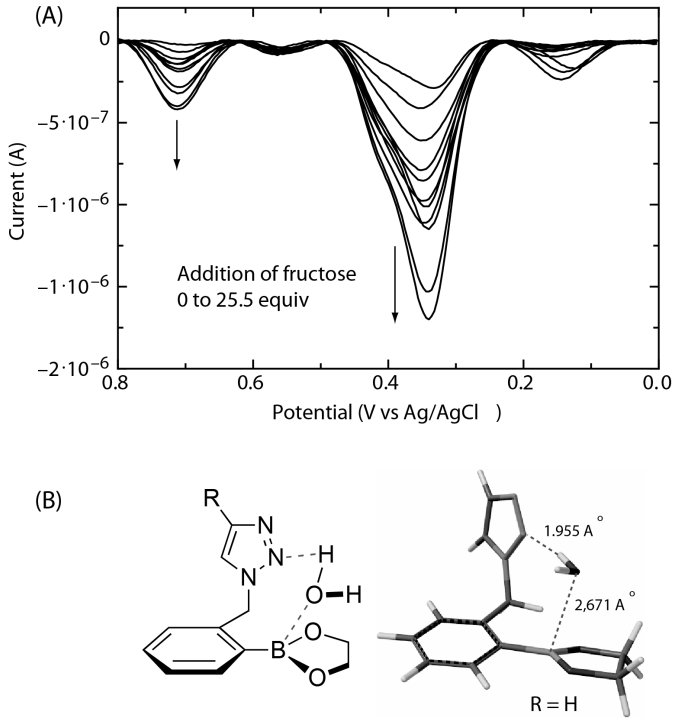

Fig. 13 (A) Differential pulse voltammetric titration of **32** (1.72 mM) with fructose in aqueous buffer/DMSO (2:1, v/v) at pH 7.4. (B) Molecular modeling of triazole-assisted complexation of phenylboronic acid and 1,2-diol in the presence of water. Calculations were done at the B3LYP/6-31G* level of theory.

CONCLUSIONS

Our recent studies have demonstrated that diphenyl-substituted TTFVs possess unique structural and electrochemical properties that render them a class of highly tunable and readily adaptable molecular building blocks for construction of a variety of functional molecular systems. Based on the redox-controlled *cis* to *trans* conformational switching of diphenyl-TTFV and the versatile reactivities of acetylenic scaffolding, sophisticated macromolecular structures with diverse topologies have been successfully prepared, including oligoyne-TTF molecular rods, TTFV-embedded conducting polymers, shape-persistent macrocycles, and functional multiple donor-chromophore ensembles. Spectroscopic and voltammetric characterizations of the new TTFV-based molecular materials have revealed intriguing applications in molecule-based optoelectronic, electrochromic, and sensory devices. At this juncture, it is envisaged that continued efforts on rational design and synthesis of new TTFV-containing systems would yield fruitful results in both synthetic and materials chemistry. On the other hand, development of a deeper understanding on the structure–property relationships for TTFV and related derivatives is still indispensable and necessary in future work, since acquisition of such fundamental knowledge will greatly accelerate the pace of finding practical applications in advanced molecular materials and devices built upon TTFV and related scaffolds.

ACKNOWLEDGMENTS

We are grateful for the financial support by the Natural Sciences and Engineering Research Council of Canada (NSERC), Canada Foundation for Innovation (CFI), and Memorial University of Newfoundland.

REFERENCES

1. F. Wudl, D. Wobschall, E. J. Hufnagel. *J. Am. Chem. Soc.* **94**, 670 (1972).
2. M. Bendikov, F. Wudl, D. F. Perepichka. *Chem. Rev.* **104**, 4891 (2004).
3. T. Murata, Y. Morita, Y. Yakiyama, K. Fukui, H. Yamochi, G. Saito, K. Nakasuji. *J. Am. Chem. Soc.* **129**, 10837 (2007).
4. Y. Kobayashi, M. Yoshioka, K. Saigo, D. Hashizume, T. Ogura. *J. Am. Chem. Soc.* **131**, 9995 (2009).
5. H. Liu, J. Li, C. Lao, C. Huang, Y. Li, Z. L. Wang, D. Zhu. *Nanotechnology* **18**, 495704 (2007).
6. C. Rovira. *Chem. Rev.* **104**, 5289 (2004).
7. O. Aleveque, P. Frere, P. Leriche, T. Breton, A. Cravino, J. Roncali. *J. Mater. Chem.* **19**, 3648 (2009).
8. A. I. de Lucas, N. Martín, L. Sánchez, C. Seoane, R. Andreu, J. Garín, J. Orduna, R. Alcalá, B. Villacampa. *Tetrahedron* **54**, 4655 (1998).
9. M. González, J. L. Segura, C. Seoane, N. Martín, J. Garín, J. Orduna, R. Alcalá, B. Villacampa, V. Hernández, J. T. López Navarrete. *J. Org. Chem.* **66**, 8872 (2001).
10. T. Enoki, A. Miyazaki. *Chem. Rev.* **104**, 5449 (2004).
11. P. Day, M. Kurmoo. *J. Mater. Chem.* **7**, 1291 (1997).
12. N. Martin, L. Sánchez, M. Á. Herranz, B. Illescas, D. M. Guldi. *Acc. Chem. Res.* **40**, 1015 (2007).
13. F. Oswald, S. Chopin, P. de la Cruz, J. Orduna, J. Garin, A. S. D. Sandanayaka, Y. Araki, O. Ito, J. L. Delgado, J. Cousseau, F. Langa. *New J. Chem.* **31**, 230 (2007).
14. B. M. Illescas, J. Santos, M. Wielopolski, C. M. Atienza, N. Martin, D. M. Guldi. *Chem. Commun.* 5374 (2009).
15. J. Santos, B. Grimm, B. M. Illescas, D. M. Guldi, N. Martín. *Chem. Commun.* 5993 (2008).
16. J. M. Williams, A. M. Kini, H. H. Wang, K. D. Carlson, U. Geiser, L. K. Montgomery, G. J. Pyrka, D. M. Watkins, J. M. Kommers. *Inorg. Chem.* **29**, 3272 (1990).
17. P. Wang, S. Bandow, Y. Maruyama, X. Wang, D. Zhu. *Synth. Met.* **44**, 147 (1991).
18. C. Loosli, C. Jia, S.-X. Liu, M. Haas, M. Dias, E. Levillain, A. Neels, G. Labat, A. Hauser, S. Decurtins. *J. Org. Chem.* **70**, 4988 (2005).
19. K. A. Nielsen, J. O. Jeppesen, E. Levillain, N. Thorup, J. Becher. *Org. Lett.* **4**, 4189 (2002).
20. E. Gontier, N. Bellec, P. Brignou, A. Gohier, M. Guerro, T. Roisnel, D. Lorcy. *Org. Lett.* **12**, 2386 (2010).
21. Y. Geng, X.-J. Wang, B. Chen, H. Xue, Y.-P. Zhao, S. Lee, C.-H. Tung, L.-Z. Wu. *Chem.—Eur. J.* **15**, 5124 (2009).
22. M. R. Bryce, W. Devonport, A. J. Moore. *Angew. Chem., Int. Ed. Engl.* **33**, 1761 (1994).
23. J. Lau, O. Simonsen, J. Becher. *Synthesis* 521 (1995).
24. D. Canevet, M. Salle, G. Zhang, D. Zhang, D. Zhu. *Chem. Commun.* 2245 (2009).
25. K. A. Nielsen, E. Levillain, V. M. Lynch, J. L. Sessler, J. O. Jeppesen. *Chem.—Eur. J.* **15**, 506 (2009).
26. P. R. Ashton, V. Balzani, J. Becher, A. Credi, M. C. T. Fyfe, G. Mattersteig, S. Menzer, M. B. Nielsen, F. M. Raymo, J. F. Stoddart, M. Venturi, D. J. Williams. *J. Am. Chem. Soc.* **121**, 3951 (1999).
27. S. Nygaard, K. C. F. Leung, I. Aprahamian, T. Ikeda, S. Saha, B. W. Laursen, S.-Y. Kim, S. W. Hansen, P. C. Stein, A. H. Flood, J. F. Stoddart, J. O. Jeppesen. *J. Am. Chem. Soc.* **129**, 960 (2007).
28. Y.-L. Zhao, W. R. Dichtel, A. Trabolsi, S. Saha, I. Aprahamian, J. F. Stoddart. *J. Am. Chem. Soc.* **130**, 11294 (2008).
29. J. Li, G. Zhang, D. Zhang, R. Zheng, Q. Shi, D. Zhu. *J. Org. Chem.* **75**, 5330 (2010).
30. B.-T. Zhao, M.-J. Blesa, F. Le Derf, D. Canevet, C. Benhaoua, M. Mazari, M. Allain, M. Sallé. *Tetrahedron* **63**, 10768 (2007).

31. J. S. Park, F. Le Derf, C. M. Bejger, V. M. Lynch, J. L. Sessler, K. A. Nielsen, C. Johnsen, J. O. Jeppesen. *Chem.—Eur. J.* **16**, 848 (2010).
32. M. Frei, F. Diederich, R. Tremont, T. Rodriguez, L. Echegoyen. *Helv. Chim. Acta* **89**, 2040 (2006).
33. T. Sugimoto, H. Awaji, I. Sugimoto, Y. Misaki, T. Kawase, S. Yoneda, Z. Yoshida, T. Kobayashi, H. Anzai. *Chem. Mater.* **1**, 535 (1989).
34. Y. Yamashita, Y. Kobayashi, T. Miyashi. *Angew. Chem., Int. Ed. Engl.* **28**, 1052 (1989).
35. P. Sandín, A. Martínez-Grau, L. Sánchez, C. Seoane, R. Pou-Amérigo, E. Ortí, N. Martín. *Org. Lett.* **7**, 295 (2005).
36. M. C. Díaz, B. M. Illescas, N. Martín, R. Viruela, P. M. Viruela, E. Ortí, O. Brede, I. Zilbermann, D. M. Guldi. *Chem.—Eur. J.* **10**, 2067 (2004).
37. M. B. Nielsen, N. F. Utesch, N. N. P. Moonen, C. Boudon, J.-P. Gisselbrecht, S. Concilio, S. P. Piotto, P. Seiler, P. Günter, M. Gross, F. Diederich. *Chem.—Eur. J.* **8**, 3601 (2002).
38. G. Chen, L. Dawe, L. Wang, Y. Zhao. *Org. Lett.* **11**, 2736 (2009).
39. G. Chen, L. Wang, D. W. Thompson, Y. Zhao. *Org. Lett.* **10**, 657 (2008).
40. Y. Yamashita, M. Tomura, M. Badruz Zaman. *Chem. Commun.* 1657 (1998).
41. Y. Yamashita, M. Tomura, S. Tanaka, K. Imaeda. *Synth. Met.* **102**, 1730 (1999).
42. T. K. Hansen, M. V. Lakshmikantham, M. P. Cava, R. M. Metzger, J. Becher. *J. Org. Chem.* **56**, 2720 (1991).
43. A. J. Moore, M. R. Bryce, A. S. Batsanov, A. Green, J. A. K. Howard, A. McKervey, P. McGuigan, I. Ledoux, E. Orti, R. Viruela, P. M. Viruela, B. Tarbit. *J. Mater. Chem.* **8**, 1173 (1998).
44. M. R. Bryce, M. A. Coffin, W. Clegg. *J. Org. Chem.* **57**, 1696 (1992).
45. R. P. Clausen, J. Becher. *Tetrahedron* **52**, 3171 (1996).
46. P. Hapiot, D. Lorcy, A. Tallec, R. Carlier, A. Robert. *J. Phys. Chem.* **100**, 14823 (1996).
47. R. Carlier, P. Hapiot, D. Lorcy, A. Robert, A. Tallec. *Electrochim. Acta* **46**, 3269 (2001).
48. A. A. O. Sarhan, C. Bolm. *Synthesis* 1000 (2009).
49. A. Ohta, Y. Yamashita. *J. Chem. Soc., Chem. Commun.* 1761 (1995).
50. D. Lorcy, J. Rault-Berthelot, C. Poriel. *Electrochem. Commun.* **2**, 382 (2000).
51. M. Guerro, T. Roisnel, P. Pellon, D. Lorcy. *Inorg. Chem.* **44**, 3347 (2005).
52. M. V. Lakshmikantham, M. P. Cava, P. J. Carroll. *J. Org. Chem.* **49**, 726 (1984).
53. Y. Yamashita, M. Tomura. *J. Solid State Chem.* **168**, 427 (2002).
54. P. Frère, A. Gorgues, M. Jubault, A. Riou, Y. Gouriou, J. Roncali. *Tetrahedron Lett.* **35**, 1991 (1994).
55. H. Müller, F. Salhi, B. Divisia-Blohorn. *Tetrahedron Lett.* **38**, 3215 (1997).
56. Y. Yamashita, M. Tomura, K. Imaeda. *Tetrahedron Lett.* **42**, 4191 (2001).
57. (a) G. Steimecke, H. J. Sieler, R. Kirmse, E. Hoyer. *Phosphor. Sulf.* **7**, 49 (1979); (b) A. J. Moore, M. R. Bryce. *Synthesis* 26 (1991).
58. C. A. Christensen, A. S. Batsanov, M. R. Bryce. *J. Org. Chem.* **72**, 1301 (2007).
59. G. Chen, I. Mahmud, L. N. Dawe, Y. Zhao. *Org. Lett.* **12**, 704 (2010).
60. G. Chen, I. Mahmud, L. N. Dawe, L. M. Daniels, Y. Zhao. *J. Org. Chem.* **76**, 2701 (2011).
61. W. A. Chalifoux, R. R. Tykwinski. *Nat. Chem.* **2**, 967 (2010).
62. P. Hascoat, D. Lorcy, A. Robert, R. Carlier, A. Tallec, K. Boubekeur, P. Batail. *J. Org. Chem.* **62**, 6086 (1997).
63. H. Enozawa, M. Hasegawa, D. Takamatsu, K.-i. Fukui, M. Iyoda. *Org. Lett.* **8**, 1917 (2006).
64. J. Massue, N. Bellec, M. Guerro, J.-F. Bergamini, P. Hapiot, D. Lorcy. *J. Org. Chem.* **72**, 4655 (2007).
65. G. Chen, S. Bouzan, Y. Zhao. *Tetrahedron Lett.* **51**, 6552 (2010).
66. J. E. Hein, V. V. Fokin. *Chem. Soc. Rev.* **39**, 1302 (2010).
67. M. Meldal, C. W. Tornøe. *Chem. Rev.* **108**, 2952 (2008).

68. J. E. Moses, A. D. Moorhouse. *Chem. Soc. Rev.* **36**, 1249 (2007).
69. K. J. Kilpin, E. L. Gavey, C. J. McAdam, C. B. Anderson, S. J. Lind, C. C. Keep, K. C. Gordon, J. D. Crowley. *Inorg. Chem.* **50**, 6334 (2011).
70. D. Schweinfurth, F. Weisser, D. Bubrin, L. Bogani, B. Sarkar. *Inorg. Chem.* **50**, 6114 (2011).
71. M. L. Gower, J. D. Crowley. *Dalton Trans.* **39**, 2371 (2010).
72. O. Fleischel, N. Wu, A. Petitjean. *Chem. Commun.* **46**, 8454 (2010).
73. S. Huang, R. J. Clark, L. Zhu. *Org. Lett.* **9**, 4999 (2007).
74. E. M. Schuster, M. Botoshansky, M. Gandelman. *Angew. Chem., Int. Ed.* **47**, 4555 (2008).
75. H. Struthers, B. Spingler, T. L. Mindt, R. Schibli. *Chem.—Eur. J.* **14**, 6173 (2008).
76. T. L. Mindt, H. Struthers, L. Brans, T. Anguelov, C. Schweinsberg, V. Maes, D. Tourwé, R. Schibli. *J. Am. Chem. Soc.* **128**, 15096 (2006).
77. Y. Hua, A. H. Flood. *Chem. Soc. Rev.* **39**, 1262 (2010).
78. S. Lee, Y. Hua, H. Park, A. H. Flood. *Org. Lett.* **12**, 2100 (2010).
79. Y. Li, A. H. Flood. *Angew. Chem., Int. Ed.* **47**, 2649 (2008).
80. A. Kumar, P. S. Pandey. *Org. Lett.* **10**, 165 (2007).
81. S. Sparapani, S. M. Haider, F. Doria, M. Gunaratnam, S. Neidle. *J. Am. Chem. Soc.* **132**, 12263 (2010).
82. A. D. Moorhouse, A. M. Santos, M. Gunaratnam, M. Moore, S. Neidle, J. E. Moses. *J. Am. Chem. Soc.* **128**, 15972 (2006).
83. T. D. James, K. R. A. S. Sandanayake, R. Iguchi, S. Shinkai. *J. Am. Chem. Soc.* **117**, 8982 (1995).
84. K. Varazo, F. Xie, D. Gulledge, Q. Wang. *Tetrahedron Lett.* **49**, 5293 (2008).
85. H. Gampp, M. Maeder, C. J. Meyer, A. D. Zuberbühler. *Talanta* **32**, 251 (1985).
86. L. Ren, Z. Liu, Y. Liu, P. Dou, H.-Y. Chen. *Angew. Chem., Int. Ed.* **48**, 6704 (2009).
87. X. Zhang, L. Chi, S. Ji, Y. Wu, P. Song, K. Han, H. Guo, T. D. James, J. Zhao. *J. Am. Chem. Soc.* **131**, 17452 (2009).
88. K. T. Kim, J. J. L. M. Cornelissen, R. J. M. Nolte, J. C. M. v. Hest. *J. Am. Chem. Soc.* **131**, 13908 (2009).
89. M. Berube, M. Dowlut, D. G. Hall. *J. Org. Chem.* **73**, 6471 (2008).
90. M. Dowlut, D. G. Hall. *J. Am. Chem. Soc.* **128**, 4226 (2006).
91. H. Cao, D. I. Diaz, N. DiCesare, J. R. Lakowicz, M. D. Heagy. *Org. Lett.* **4**, 1503 (2002).
92. K. Mulla, P. Dongare, N. Zhou, G. Chen, D. W. Thompson, Y. Zhao. *Org. Biomol. Chem.* **9**, 1332 (2011).
93. G. Wulff. *Pure Appl. Chem.* **54**, 2093 (1982).
94. M. Lauer, G. Wulff. *J. Organomet. Chem.* **256**, 1 (1983).
95. L. Zhu, S. H. Shabbir, M. Gray, V. M. Lynch, S. Sorey, E. V. Anslyn. *J. Am. Chem. Soc.* **128**, 1222 (2006).

